

Microcoil High-Resolution Magic Angle Spinning NMR Spectroscopy

Hans Janssen, Andreas Brinkmann, Ernst R. H. van Eck, P. Jan M. van Bentum, and Arno P. M. Kentgens*

Department of Physical Chemistry/Solid-State NMR, Institute for Molecules and Materials, Radboud University Nijmegen, Toernooiveld 1, 6525 ED Nijmegen, The Netherlands

Received February 25, 2006; E-mail: a.kentgens@nmr.ru.nl

We present a new technique that combines the versatility of magic angle spinning (MAS) nuclear magnetic resonance (NMR) spectroscopy with the superior sensitivity provided by very small detection coils. This opens the way for NMR studies of solid samples with nanoliter volumes. Furthermore, the very strong radio frequency (rf) fields that can be generated by these microcoils facilitate a much broader excitation bandwidth and/or decoupling efficiency.

Although solid-state NMR is the method of choice for investigating local structure, alignment, and dynamics of nonsoluble and noncrystalline functional materials, its feasibility for studying chemically and biologically relevant systems is often hampered by sensitivity. For sensitivity reasons, microcoil technology was introduced in liquid-state NMR for mass-limited samples¹ and high-resolution, small-volume MRI experiments², based on the observation that the efficiency of a solenoid coil scales inversely with its diameter.^{1,3} By reciprocity, this also allows the generation of very high rf fields with limited amount of power, which has been exploited for static wide-line NMR studies in solids.⁴

Two important pillars underpin the success of solid-state NMR as an analytical tool in materials science: first, sample rotation about the so-called “magic angle”⁵ needed to average anisotropic contributions to the resonance lines and second, polarization transfer from abundant nuclei (e.g., protons) to less-abundant nuclei with low gyromagnetic ratios such as ¹³C or ¹⁵N.^{6,7} The evolution of a variety of techniques for studying internuclear distances, bond angles, molecular orientation and dynamics, spin diffusion, and chemical exchange processes, is built on these foundations.

Here we describe a microMAS design, featuring microcoil-based resonators with either 400/300 μm outer/inner diameter or 335/235 μm outer/inner diameter coils and sample holders down to 170/125 μm outer/inner diameter (10 nL sample volume), mounted on a regular commercially available MAS unit (Figure 1). The microcoil resonator is a solenoid coil integrated into a capacitor similar to that developed for static experiments⁴ leaving a 220 μm opening (30 nL internal volume) for the rotor. The advantage of this design is its mechanical stability and minimization of signal losses. Compared to regular millimeter-sized coils with only a few windings, our microcoil design with over 10 windings allows for a better B₁ homogeneity over the sample volume, thus improving efficiency. Using microcoils, susceptibility broadening can be a serious issue that limits the resolution. In the present design, this is not the case, as these effects are averaged by MAS. The resolution of most solids spectra is, therefore, determined by the intrinsic spin interactions in the materials. Low-rf-power operation combined with the fact that only a small homogeneous B₀ volume is needed may help to fulfill the promise of tabletop NMR equipment. Low-power requirements and the absence of frictional heating in combination with the advantageous surface/volume ratio, which results in better cooling efficiency, can alleviate heating

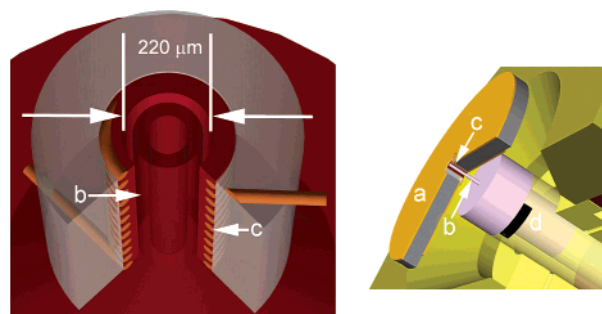


Figure 1. Schematic of the microMAS circuit consisting of a capacitor (a) with embedded microcoil (c) and rotor (b) piggy-backed onto a 4-mm Chemagnetics MAS stator. The microMAS sample container is precision machined from Vespel and can be fitted in the 4-mm MAS rotor (d).

problems in, for example, hydrous biological samples with high salt concentrations such as membranes. In the present contribution, we focus on the feasibility of using microcoil circuits to study mass-limited (bio)organic compounds using CP-MAS.

A critical step in the probe assembly is the alignment of the microcoil circuit with respect to the rotor axis. Nevertheless, we found spinning to be very stable without any sizable excursions of the rotation axis; as a result, the attainable spinning speeds are those imposed by the supporting rotor, being 2–15 kHz for the 4 mm design used here. The spinning axis was set to the magic angle using KBr;⁸ in the latest design the 4-mm support rotor is fitted with a separate circuit tuned for ⁷⁹Br observation. In this way, one can quickly set the spinning axis to the magic angle and immediately proceed with the measurement of interest without the need of changing the sample. This approach makes simultaneous acquisition of spectra from samples in both the 4-mm rotor and the microrotor possible, thus allowing for efficient use of instrument time.

A cross-polarization (CP) experiment was performed at 14.1 T (600 MHz) using 6 nL of 25% C₂-enriched glycine in the microrotor spinning at 8.2 kHz. The line width of the C₂-resonance is 117 Hz, identical to the line width in a commercial probe. This demonstrates that MAS can spin out residual line broadenings due to susceptibility effects. A spectrum with a S/N = 61.5 ($I_{\max}/\sigma_{\text{noise}}$) was obtained in 10 800 scans. Although further work is needed to assess the exact sensitivity of the probe head, this shows the feasibility of getting CP-MAS spectra for minute sample quantities in a reasonable amount of time. A first assessment of the sensitivity shows that the circuit is not performing at the theoretical optimum yet, leaving room for further improvements in the circuit design. The microcoil circuit allowed the generation of a proton decoupling field (expressed as nutation frequencies ($\gamma B_1/2\pi$) in Hz) of 200 kHz with as little as 1.35 W of rf power. As the circuits are designed to handle hundreds of watts of power, one can generate rf fields well beyond the capabilities of commercial CP-MAS probes. This is shown for a uniformly ¹³C-labeled trialanine sample in antiparallel β -sheet form.⁹ Its CP-MAS spectrum obtained in the microrotor,

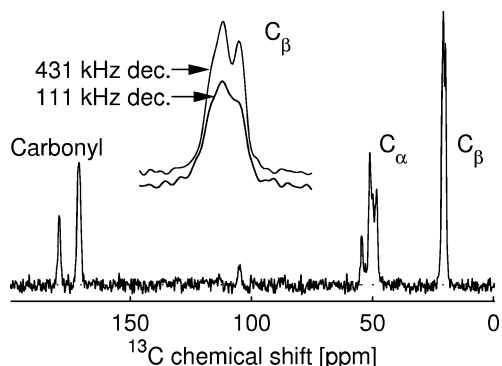


Figure 2. ^{13}C CPMAS spectrum for uniformly ^{13}C -labeled trialanine in antiparallel β -sheet form, adding 10 240 acquisitions. Inset: the C_β region shows improved resolution when using a CW-decoupling field strength of 431 kHz, as compared to 111 kHz.

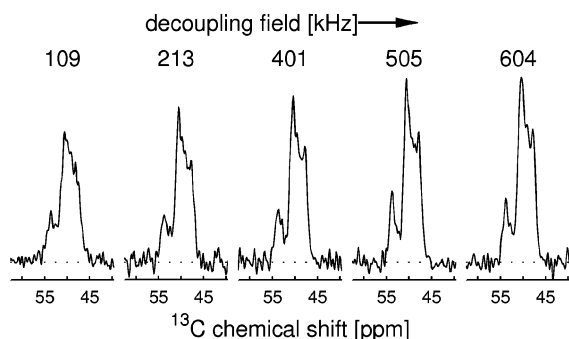


Figure 3. C_α region of a ^{13}C CP-MAS spectrum of uniformly ^{13}C -labeled trialanine (in antiparallel β -sheet form) as a function of proton CW decoupling strength. The increasing intensity is a result of line narrowing due to increasing decoupling efficiency.

spinning at 10 kHz at 14.1 T, is shown in Figure 2 and is comparable to a regular CP-MAS spectrum. Coherent averaging processes in NMR critically depend on the time scales of the averaging process with respect to the NMR interactions. Ideally, these should differ by an order of magnitude. Indeed, increasing the proton rf power during decoupling shows improved efficiency of the continuous wave (CW) decoupling, for example, the C_β carbons show better line separation at high decoupling fields (Figure 2). Increasing the decoupling rf field strength up to 600 kHz, using the 335/235 μm coil, we observe an increasing intensity for the C_α carbons as a result of the narrowing of the resonances, which levels off at 500 kHz decoupling (Figure 3).

Target applications for microMAS are mass-limited samples. These do not only include samples whose absolute quantity is restricted, but also materials which under specific conditions occur in complex molecular arrangements such as fibrous proteins (e.g., silks or amyloid proteins) or self-assembled biomimetic materials. For oriented samples, NMR can provide detailed information about the molecular arrangement of the various building blocks. As a proof of principle, we studied a silk rod prepared from the *Bombyx mori* silk gland¹⁰ with 20% ^{13}C enrichment of the carbonyl groups of the glycine residues. The ^{13}C CP-MAS spectrum of the fine silk rod is shown in Figure 4a for a spinning speed of 8.2 kHz. The carbonyl peak is very broad (~ 1 kHz), indicating a wide distribution in isotropic chemical shifts, indicative for great structural disorder in the silk rod. In a systematic study of ^{13}C CSA tensors in peptides, an isotropic shift variation of 7 ppm was observed for glycine residues.¹¹ The silk sample consists mainly of (Ala–Gly–Ser–Gly–Ala–Gly)_n in the form of silk I, random coil, and silk II (mainly antiparallel β -sheet). MAS spectra of a single silk fibril

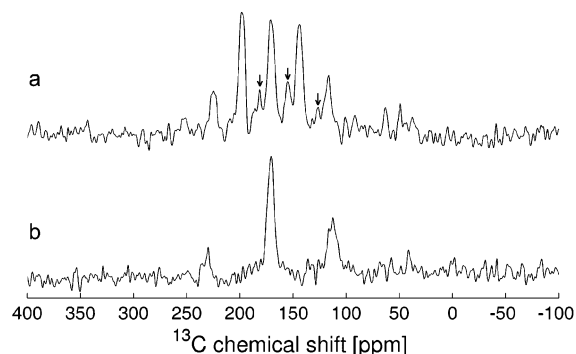


Figure 4. ^{13}C CP-MAS spectra of a single silk rod drawn from the silk gland of *Bombyx mori* with approximate dimensions of 50 μm \times 800 μm , spinning at 4 kHz (a) and 8.2 kHz (b) using a 400/300 μm coil. At 8.2 kHz spinning (108 000 scans), the spectrum is dominated by a 1 kHz broad carbonyl resonance at 171 ppm, accompanied by two spinning sidebands. At 4 kHz spinning (348 164 scans), the spinning sidebands are more prominent. The arrows indicate the spinning sideband pattern from the Vespel rotor material.

will give information about the preferential orientation of the crystalline regions in the fibril. Analysis of the spinning sideband pattern of the spectrum obtained at 4 kHz MAS (Figure 4b) gives $\sigma_{11} = 247$ ppm, $\sigma_{22} = 176$ ppm, and $\sigma_{33} = 89$ ppm, that is, the full carbonyl tensor,¹¹ so we conclude that there is no sign of preferential orientation of the crystalline units in the fibril. When its large line width and moderate level of enrichment is considered, this silk rod is a demanding application in terms of sensitivity.

In conclusion, we have shown that high-resolution solid-state NMR can be miniaturized to study samples in the nanoliter regime. We implemented a viable microdesign that incorporates cross-polarization and MAS, which is an essential step to optimize high-resolution solid-state NMR for mass-limited samples. Furthermore, this microdesign can either operate at extremely low rf power or generate extremely high rf fields, helping to excite broad spectra and achieve highly efficient proton decoupling, thus, substantially improving spectral resolution.

Acknowledgment. The authors are very grateful to Prof. T. Asakura and Dr. K. Yamauchi (Tokyo University of Agriculture and Technology) for supplying the silk rod and trialanine samples and for their interest in this work. We thank Jan van Os and Gerrit Jansen for their technical support and discussions. Edwin Sweers is acknowledged for his (micro)mechanical craftsmanship.

Supporting Information Available: Materials, experimental NMR procedures, and glycine CPMAS spectra (PDF). This material is available free of charge via the Internet at <http://pubs.acs.org>.

References

- (1) Olson, D. L.; Peck, T. L.; Webb, A. G.; Magin, R. L.; Sweedler, J. V. *Science* **1995**, *270*, 1967.
- (2) Ciobanu, L.; Webb, A. G.; Pennington, C. H. *Prog. Nucl. Magn. Reson. Spectrosc.* **2003**, *42*, 69.
- (3) Hoult, D. I.; Richards, R. E. *J. Magn. Reson.* **1976**, *24*, 71.
- (4) Yamauchi, K.; Janssen, H. J. M.; Kentgens, A. P. M. *J. Magn. Reson.* **2004**, *167*, 87.
- (5) Andrew, E. R.; Bradbury, A.; Eades, R. G. *Nature* **1958**, *182*, 1659.
- (6) Pines, A.; Gibby, M. G.; Waugh, J. S. *J. Chem. Phys.* **1973**, *59*, 569.
- (7) Stejskal, E. O.; Schaefer, J. *J. Am. Chem. Soc.* **1976**, *98*, 1031.
- (8) Frye, J. S.; Maciel, G. E. *J. Magn. Reson.* **1982**, *48*, 125.
- (9) Asakura, T.; Okonogi, M.; Nakazawa, Y.; Yamauchi, K. *J. Am. Chem. Soc.* **2006**, *128*, 6231.
- (10) Zhao, C.; Asakura, T. *Prog. Nucl. Magn. Reson. Spectrosc.* **2001**, *39*, 301.
- (11) Wei, Y.; Lee, D.-K.; Ramamoorthy, A. *J. Am. Chem. Soc.* **2001**, *123*, 6118.

JA061350+